Ca^{2+} Imaging With Two-photon Microscopy to Detect the Disruption of Brain Function in Mice Administered With Neonicotinoid Insecticides

Anri Hirai
Hokkaido University
Shouta Sugio
Nagoya University
Collins Nimako
Hokkaido University
Shouta Nakayama
Hokkaido University
Keisuke Kato
Toho University
Keisuke Takahashi
Toho University
Koji Arizono
Kumamoto University
Tetsushi Hirano
University of Toyama
Nobuhiko Hoshi
Kobe University
Kazutoshi Fujioka
Albany College of Pharmacy and Health Sciences
Kumiko Taira
Tokyo Women's Medical University
Mayumi Ishizuka
Hokkaido University
Hiroaki Wake
Nagoya University
Yoshinori IKENAKA (y_ikenaka@vetmed.hokudai.ac.jp)
Hokkaido University

Research Article

Keywords: Neonicotinoid pesticides, untargeted effects, median lethal dose, two-photon microscope

Posted Date: May 19th, 2021

DOI: https://doi.org/10.21203/rs.3.rs-484024/v1

Version of Record: A version of this preprint was published at Scientific Reports on March 24th, 2022. See the published version at https://doi.org/10.1038/s41598-022-09038-7.

Abstract

Neonicotinoid pesticides are insecticides that are insecticides that reportedly have untargeted effects on bees and dragonflies causing a reduction in numbers. Neonicotinoids act as neuroreceptor modulators, and some studies have reported their association with neurodevelopmental disorders. However, the effect of neonicotinoids on the central nervous system has not yet been identified. Herein, we conducted *in vivo* Ca^{2+} imaging using a two-photon microscope to detect abnormal activity of neuronal circuits in the brain using a neonicotinoid. The oral administration of acetamiprid (ACE) (20 mg/kg body weight [bw]) in mature mice with a less than the no-observed-adverse-effect level (NOAEL) and a tenth or half of the median lethal dose (LD_{50}) of nicotine (0.33 or 1.65 mg/kg bw, respectively), as a typical nAChRs agonist, increased anxiety-like behavior associated with altered activities of the neuronal population in the somatosensory cortex. Furthermore, we detected ACE and metabolites in the brain 1 h after ACE administration. The results suggested that *in vivo* Ca^{2+} imaging using a two-photon microscope enabled the highly sensitive detection of neurotoxicant-mediated brain disturbance of nerves.

Introduction

Neonicotinoid (NN) pesticides are one of the causes of mass bee deaths and drastic reduction in the number of red dragonflies. They were introduced in the 1990s and are currently the most widely used pesticides worldwide. In addition to their impact on the environment, some recent studies have reported their effect on humans that are particularly associated with neurodevelopmental disorders[1]. Therefore, environmental groups and researchers have been calling for the imposition of stricter regulations and appropriate impact assessments. In contrast, some studies have highlighted the safety of NNs as they reportedly have a lower affinity for mammalian nicotinic acetylcholine receptors (nAChRs) than for those in insects[2]. However, a recent *in vivo* study found an increase in anxiety-like behavior during the elevated plus-maze (EPM) test in mice exposed to clothianidin, one of the most popular NNs, below the no-observed-adverse-effect level (NOAEL)[3]. NNs have been detected in the urine of Japanese people without occupational exposure[4,5]. Researchers have reported a correlation between the detection rate of NN in urine and the domestic shipment volume in Japan of some NNs, such as thiamethoxam[4]. In addition, dm-ACE (acetamiprid), an ACE metabolite, has been detected in the urine of extremely low-birth-weight infants, collected within 48 h and 14 days after birth[6]. The aforementioned findings suggest that humans may be chronically exposed to NNs, despite not being engaged in NN-associated occupations, such as agriculture. NNs exert their effects by modulating nAChRs at low concentrations without causing histopathological changes[3]. This eventually affects emotional and cognitive behaviors. Since it is difficult to assess the effects of NNs on emotional and cognitive behaviors in higher mammals such as humans, it is necessary to understand the mechanism of action of chemical substances and conduct appropriate toxicological effect assessment. However, the mechanism of neurotoxicity of NNs is still not understood in detail.

Behavioral tests (e.g., EPM test, social interaction test, and tail-flick test) facilitate the assessment of the neurotoxicity of chemicals. However, these hierarchical tests do not always provide adequate assessment strategies to evaluate the effects that may become apparent after growth[7]. Current toxicity test methods, such as the Developmental Neurotoxicity Study (OECD TG426) defined by the Organization for Economic Cooperation and Development, are insufficient to detect disturbances in higher brain functions, such as developmental neurotoxicity and cognitive impairment. This is because OECD TG426 requires large-scale animal experiments[7,8].

This necessitates the development of novel and sensitive detection techniques to clarify the mechanisms of neurotoxicity caused by exposure to low concentrations.

Two-photon microscopy utilizes laser scanning, enabling the visualization of the function and construction of neurons in living awake animals. The somatosensory cortex is located in the anterior part of the parietal lobe and contributes to higher sensory functions by integrating signals received from sensory receptors and perceiving them as meaningful information[9,10]. The α4β2 and α7 subtypes are the commonly expressed nAChRs[10,11]. The information received by the sensory organs is relayed to the brain, processed, and then reintegrated. The details of this reintegration mechanism have not yet been elucidated. Nonetheless, the firing frequency, firing patterns, synchronized firing, and other factors presumably play a role in coding information and making connections between the segmented information and the information itself[12–15]. nAChRs are expressed on inhibitory neurons and suppress the excitatory neurons and inhibitory cells that inhibit the excitatory cells[16,17]. For example, inhibitory neurons, such as vasoactive intestinal peptide (VIP)-expressing cells, somatostatin (SOM)-expressing cells, parvalbumin (PV)-expressing cells, and excitatory neurons, such as pyramidal cells, are distributed in the prefrontal cortex. The aforementioned receptors are not expressed in pyramidal cells. However, the α5, α7 and β2, and α7subtypes are reportedly expressed in VIP-, SOM-, and PV-expressing cells[18]. The VIP-expressing cells inhibit SOM- and PV-expressing cells. Furthermore, the SOM- and PV-expressing cells inhibit pyramidal cells[18]. VIPs, SOMs, and pyramidal cells are also expressed in layers II/III of the somatosensory cortex[19]. In other words, nAChRs agonists may alter neural activity in the somatosensory cortex and affect emotional cognitive behavior.

We selected ACE among other NNs because of its use worldwide and the ease of detection of ACE and metabolites in the human urine. Acute neurotoxicity studies on ACE evaluation have not been conducted in mice. The lowest NOAEL calculated in toxicity tests was 20.3 mg/kg/day in an 18-month carcinogenicity test[20,21]. The lowest-observed-adverse-effect level (LOAEL) and NOAEL in mice in a general pharmacological study of the central nervous system were 20 mg/kg and 10 mg/kg, respectively, and a decrease in spontaneous locomotor activity was observed at the LOAEL level[21]. In light of these factors, the dose concentration of ACE in this study was set at 20 mg/kg. Following the study of Kimura-Kuroda et al. (2012), we also administered nicotine as a typical nAChRs agonist and tried to compare it with ACE. Since nicotine is a positive control, we administered nicotine at two different concentrations, 1/2 or 1/10 of the oral LD_{50}, and examined the changes at high or low concentrations.

The study had three objectives: 1. To evaluate the neurotoxicity of ACE using the EPM test in mice; 2. To examine the neuronal activity in the somatosensory cortex of mice; and 3. To determine the levels of ACE and its metabolites in mice brain. Further, we attempted to detect disturbances in brain function by examining changes in their behavior and neuronal activity through behavioral tests and Ca^{2+} imaging using two-photon microscopy. We also quantified the concentrations of ACE and its metabolites in the brain and blood to determine if ACE localizes to specific areas of the brain.

Materials And Methods

Chemicals

ACE was purchased from Cosmo Bio Co., Ltd. (100% purity, Tokyo, Japan) and Kanto Chemical Co., Inc. (Tokyo, Japan). ACE-d6 and *N*-desmethyl-acetamiprid-d3 were purchased from Hayashi Pure Chemical Industries, Ltd.

(Osaka, Japan). Acetamiprid-N-desmethyl (dm-ACE) was purchased from Sigma-Aldrich (St. Louis, MO, USA). *N*-descyano-acetamiprid (dc-ACE), *N*-desmethyl-descyano-acetamiprid (dm-dc-ACE), *N*-acetyl-acetamiprid (*N*-acetyl-ACE), and *N*-acetyl-desmethyl-acetamiprid (*N*-acetyl-dm-ACE) were synthesized by the Toho University. Nicotine (97% purity), isoflurane, formic acid (99% purity), acetic acid (99.7% purity), and sodium acetate (98.5% purity) were purchased from Fujifilm Wako Pure Chemicals Co., Inc. (Tokyo, Japan). Moreover, we purchased magnesium sulfate from Agilent Technologies (Tokyo, Japan). All other reagents were purchased from Kanto Chemical Co., Inc. (Tokyo, Japan).

Treatments of animals with acetamiprid and nicotine

All study was conducted in accordance with the Experimental Committee of the Faculty of Veterinary Medicine, Hokkaido University, Japan. All animal experiments were performed in accordance with the Guide for the Care and Use of Laboratory Animals, in conformity with the Association for the Assessment and Accreditation of Laboratory Animal Care International (AAALAC; approval number: 18-0061). Male C57BL/6J mice (7 weeks old) were obtained from CLEA Japan, Inc. (Tokyo, Japan) and kept in a 12 h light/dark cycle at a room temperature of 22±1 °C and humidity of 70±5%. The mice were provided food (breeding solid feed for mice, rats, and hamsters: CE-2, CLEA Japan, Inc., Tokyo, Japan) and tap water ad libitum. We changed the feed and water twice a week. The mice cages were changed once a week. Following a 1-week acclimation period, we randomly divided the mice into four groups: the control group (group C), ACE group (group A), low concentration nicotine group (group L), and high concentration nicotine group (group H). ACE was dissolved in distilled water (DW) to 2 mg/mL, and nicotine to 0.033 mg/mL or 0.165 mg/mL. At 9 weeks of age, we orally administered DW, ACE (20 mg/kg bw), low-dose nicotine (0.33 mg/kg bw), and high-dose nicotine (1.65 mg/kg bw) to groups C, A, L, and H, respectively, in an aware manner under isoflurane anesthesia. Sonde (FUCHIGAMI Co., Ltd., Kyoto, Japan) was used to administer a 10 mL/kg bw dose. The ACE dose used in the current study was inferred from the NOAEL of the ACE[21]. Furthermore, the nicotine dose was based on the oral LD_{50} of mice, described in the International Peer Reviewed Chemical Safety Information[23], and was calculated as 1/10 and 1/2 LD_{50}. Approximately 1 h after administration, we subjected the mice to the EPM test. Groups C (n=5) and A (n=8) were then euthanized, dissected, and sampled. We conducted euthanasia via cervical dislocation under deep isoflurane anesthesia. At necropsy, whole blood and organs, such as the cerebral cortex, hippocampus, striatum, and liver, were collected and stored at -20 °C.

EPM test

The EPM comprises walled (closed arms) and wall-less passages (open arms) (two each). This behavioral test uses the equilibrium between curiosity in a novel environment and fear of heights as a measure of anxiety-like behavior[24,25]. Following chemical administration, the EPM test was performed after keeping the mice in a dark room for 1 h, for groups C, A, L, and H (n=8 each, in accordance with the previous study[26]). The EPM apparatus (length, 29.5 cm; width, 6 cm; wall height, 15 cm; and height, from floor; 41.5 cm) was set up high off the floor such that the closed arms and open arms were at a 90° angle. The brightness of the light within the apparatus was set at 20 lx. Each mouse was allowed to move freely for 5 min in the EPM device. We conducted the behavioral analysis using Smart 3.0 (PHILIPS, s/n: DCF76-90C, Nihon Bioresearch Inc., Gifu, Japan).

Ca^{2+} imaging using two-photon microscopy

The brains of different sets of mice from all groups were surgically operated at 8 weeks of age and used for Ca^{2+} imaging. At 10 weeks of age, we orally administered DW, ACE (20 mg/kg bw), low-dose nicotine (0.33 mg/kg bw), and high-dose nicotine (1.65 mg/kg bw) to the groups C, A, L, and H, respectively. We subsequently subjected them to *in vivo* $Ca2^{+}$ imaging.

We placed a fixation plate on the heads of the mice to perform an *in vivo* imaging of the central nervous system. The mice were anesthetized by an intraperitoneal administration of ketamine (74 mg/kg) and xylazine (10 mg/kg). Following shaving and disinfection of the parietal area, we incised the skin and exposed and cleaned the skull. Moreover, a custom-made metal plate was fixed to the skull using dental cement (G-CEM ONE; GC Co., Ltd., Gifu, Japan). The exposed skull was coated with acrylic-based dental resin cement (Super Bond; Sun Medical, Shiga, Japan).

After 1 day of recovery, the animals were subjected to craniotomy and inoculation with adeno-associated virus vectors. We immobilized the mice with a fixation plate in a stereotaxic instrument (SR-5M-HT, NARISHIGE, Tokyo, Japan) under isoflurane (1%) anesthesia. The skull above the somatosensory cortex (1.2 mm caudal to the cross suture and 1.5 mm lateral to the cross suture) was sectioned into a circle (2 mm in diameter) using a dental drill. The brain surface was exposed to craniotomy (Masamizu et al., 2014). We used an adeno-associated viral vector expressing GCaMP6f, a neuron-specific fluorescent calcium indicator protein, adeno-associated virus 1-hSyn-GCaMP6f (Addgene), to visualize the neuronal activity in layers II/III of the cerebral cortex. We connected a glass pipette ((tip diameter: 10 μm) DGC-1; NARISHIGE, Tokyo, Japan) filled with diluted viral vector solution (1.0×1012 viral gram/mL) to a motorized microinjector (IM-31; NARISHIGE, Tokyo, Japan). The tip of the glass pipette was inserted at a depth of 250 μm from the brain surface, and 500 nL of the viral vector solution was injected. Following the injection, the glass pipette was held for 10 min and then withdrawn. This prevented a leakage of the viral vector solution. The virus vectors were inoculated at three locations within the craniotomy window. Following inoculation, a custom-made circular cover glass (Matsunami Glass Ind., Ltd., Osaka, Japan) was crimped to the craniotomy position. The edges of the glass were fixed with dental cement and dental resin cement to create the observation window.

In vivo Ca^{2+} imaging using two-photon microscopy

We used two-photon microscopy (objective lens: × 10, XLPlan, NA 1.0, Zeiss, Tokyo, Japan; microscope; LSM 7 MP, Zeiss, Tokyo, Japan) and two-photon excitation laser (wavelength 950 nm. Ti: sapphire Chameleon Ultra II Laser; Coherent, Tokyo, Japan) for the *in vivo* Ca^{2+} imaging of neurons, distributed 200-250 μm deep from the brain surface. The mice were held on a dedicated fixation platform, placed under an objective lens. We conducted the imaging under wakefulness. The imaging frame was of 512 × 512 pixels (207.94 μm × 207.94 μm). We set the image acquisition speed to 0.39 s/frame (0.39 s/frame) and captured 1000 frames of continuous images (approximately 6 min). The imaging was performed for group A (n=2), L (n=4), and H (n=3) before chemical administration and 30 min or 2 h after chemical administration. The mice were continuously fixed on the microscope until the time of imaging (30 min after chemical administration) and returned to their cages for imaging 2 h later (Fig. 2A).

To further study the brain activity, we performed *in vivo* Ca2+ imaging using two-photon microscopy. We attempted to associate the population activity of neurons detected by behavioral changes or the high sensitivity of *in vivo* Ca^{2+} imaging for NNs in the brain. We measured and quantified the frequency and area under the curve (AUC) (see also Methods) of the Ca^{2+} transients in single neurons, and the correlation among activity in single neurons within the neuronal population (the C.C.) before, 30 min, and 2 h after the administration of ACE and nicotine (low and high concentration). We initially determined the nature of the neurons expressing GCaMP6f, driven by the synapsin promoter (Fig. 2A, B) (total of 79, 43, and 84 cells in groups A, L, and H, respectively). We divided the neurons with high (high-AUC cell group) and low spontaneous activity (low-AUC cell group). We then compared the properties of Ca^{2+} transients in each group (Fig. 2C, H, M).

Imaging analysis

We used Fiji Image J (1.53e; NIH, Java 1.8.0_172; 64 bit)[27] and MATLAB® R2019b (The MathWorks, Inc., Natick, MA, United States) to analyze the imaging data. TurboReg[28] was used to compensate for the displacement of the focal plane. We used a semi-automatic algorithm to correlate the fluorescence intensity between adjacent pixels to define the region of interest (ROI) around the cell. The ROI was visually confirmed. The fluorescence in the ROI was averaged over time, and background fluorescence was subtracted. We detected a Ca^{2+} response when the fluorescence intensity was two standard deviations (SD) above the mean baseline.

In the acute exposure experiment, we analyzed the cells that were commonly observed in all images captured before, 30 min, and 2 h after the administration. In contrast, we analyzed all cells observed in each image in the subacute exposure experiment.

Sample preparation for liquid chromatography/mass spectrometry (LC/MS) analysis of ACE and its metabolites

We conducted the pretreatment for LC/MS analysis using different methods for the organs and blood. We extracted and purified ACE and its metabolites from tissues using the QuEChERS method (Anastassiades et al., 2003; Lehotay et al., 2007; Liu et al., 2011). Approximately 10 mg of tissue samples obtained from the target organs were weighed into 1.5 mL tubes. We then added 1 mL acetonitrile containing 1% acetic acid and a 50 µL internal standard master mix containing acetamiprid-d6 and dm-acetamiprid-d3 (100 ppb) to the tissue sample. The samples were homogenized using a TissueLyser (1 min, 30/s; Retsch, QIAGEN K.K., Tokyo, Japan) and two zirconia beads (2.0 mm; Tokyo Garasu Kikai Co., Ltd., Tokyo, Japan). Following homogenization, the tissue homogenate was centrifuged at 10,000 g for 5 min. The supernatant was carefully transferred to a 15 mL tube. Subsequently, we added 3 mL of sodium acetate buffer (0.1667 g/mL), 2 mL DW, and 4 g magnesium sulfate (MgSO4) to the supernatant. The sample was vortexed thoroughly and centrifuged at 10,000 g for 10 min. We eventually diluted a 20 µL aliquot of the supernatant in 180 µL of DW, containing 1% formic acid. It was then subjected to LC-MS/MS analysis.

We prepared the blood specimens by measuring 50 µL of whole blood into a 1.5 mL tube and topping up to the 1.5 calibrated mark using DW. The extraction and purification process of the blood samples followed a similar QuEChERS protocol adopted for tissue samples (as explained before). However, we diluted 100 µL of the supernatant from whole blood extract in 100 µL of DW, containing 1% formic acid for LC/MS in the final stage.

LC/MS analysis

We quantified the concentrations of ACE and its metabolites from the extracts of tissues and whole blood using an Agilent 1290 Infinity ultra-high performance liquid chromatography system (Agilent Technologies, Tokyo, Japan), coupled with an Agilent 6495 triple quadrupole mass spectrometer (Agilent Technologies, Tokyo, Japan). The UK Phenyl HT column measured 150×2 mm and 3.0 μm particle size (Intact, Kyoto, Japan). The temperature was set at 60 °C. We used DW containing 0.1% formic acid and 10 mM ammonium acetate as the mobile phase A. In contrast, methanol containing 0.1% formic acid and 10 mM ammonium acetate was used as phase B. The analytes were separated at a flow rate of 0.6 mL/min. The gradient was initiated at 1% B, increased linearly to 95% B from 0.5 min to 4 min, maintained at 95% B for 5 min, returned to 1% B, and equilibrated for 5.5 min before the next injection. The injection volume was 20 μL. Furthermore, we conducted the ionization using the positive mode of the electrospray ionization (ESI) method. Table 1 summarizes the retention times (RT), multiple reaction monitoring (MRM) transitions, and collision energies (CE) for each analyte.

We performed the quantification using the internal standard method. Seven calibration points were used to plot the standard curves for quantification, and the average coefficient of determination was >0.99. We calculated the limit of quantification (LOQ) and limit of detection (LOD) of the analytes as 10×SD/S and 3.3×SD/S, respectively (Table 2). While SD represents the standard deviation of the five repetitions of the standard solution, S represents the slope of the calibration curve. We checked the peak shape for the analysis. A peak with a signal-to-noise ratio >10 was adopted as the peak.

Statistical analyses

We conducted statistical analyses using Excel (2016) and JMP® (SAS Institute Inc., Cary, NC, USA). While we performed the Steel test to analyze the Ca^{2+} imaging results, the Dunnett's test was used to analyze the behavioral test results. The Steel test was only used for the distance traveled in open arms and the total distance traveled in the acute exposure study. Data are presented as the mean ± standard error, and the significance level was set at $p<0.05$.

Results

EPM test

We measured the percentage of distance traveled and the time spent in each arm, the number of entries, the number of moves between the zones, and the total distance traveled (Fig. 1).

The distance traveled in the open arms was 25.3 ± 3.8%, 22.8 ± 6.6%, 22.7 ± 4.3%, and 13.1 ± 3.7% for groups C, A, L, and H, respectively (Fig. 1A); the time spent in the open arms was 32.9 ± 4.6% for group C, 27.8 ± 7.5% for group A, 31.3 ± 5.5% for group L, and 15.9 ± 4.6% for group H (Fig. 1C). The number of entries was 24.0 ± 2.8, 15.4 ± 1.6, 17.9 ± 1.8, and 9.6 ± 3.0 for groups C, A, L, and H, respectively (Fig. 1E). There was a significant difference in the number of entries for groups A and H compared to that for group C (p=0.0365 and 0.0006, respectively).

The distance traveled in the closed arms in groups C, A, L, and H was 55.6 ± 3.7%, 61.2 ± 6.4%, 58.3 ± 4.0%, and 74.4% ± 4.4%, respectively (Fig. 1B). The time spent was 42.3 ± 4.1% for group C, 53.7 ± 7.5% for group A, 45.5 ± 4.6% for group L, and 68.7 ± 6.5% for group H (Fig. 1D), with a significant increase for group H (p=0.0293 and

0.0103). In contrast, the number of entries for groups C, A, L, and H was 22.8 ± 1.6 times, 18.4 ± 2.3 times, 18.0 ± 1.8 times, and 18.6 ± 2.7 times, respectively (Fig. 1F), thus showing no significant difference.

The number of moves between the zones was 93.3 ± 5.7 times, 67.4 ± 7.3 times, 71.8 ± 4.3 times, and 56.3 ± 11.0 times for groups C, A, L, and H, respectively (Fig. 1G), with a significant decrease in groups A and H (p=0.0417 and 0.004, respectively). The total distance traveled in groups C, A, L, and H was 1119 ± 46.7 cm, 988.6 ± 89.7 cm, 978 ± 55.3 cm, and 1003 ± 97.8 cm, respectively (Fig. 1H), with no significant difference.

Ca^{2+} imaging using two-photon microscopy

The frequency and amplitude of Ca^{2+} transients and the cross-correlation (C.C.) of the neuronal population were measured (Table 4).

The amplitude of Ca^{2+} transients had significantly decreased in the high-AUC cell group, 30 min and 2 h after ACE administration (Fig. 2D). In contrast, it had increased in the low-AUC cell group, 30 min after high-dose nicotine administration (Fig. 2N). However, low-dose nicotine administration did not generate any detectable changes (Fig. 2I). Following NNs administration, the frequency of Ca^{2+} transients did not alter in any cell group (Fig. 2E, 2J, and 2O). The C.C. of the neuronal population had significantly decreased and increased in all high-AUC cell and low-AUC groups, respectively, 30 min and 2 h after NNs administration (Fig. 2F, 2K, and 2P). Our results indicate that nicotine perturbs the synchronization of a specific neuronal population, with lesser effects on the amplitude and frequency of Ca^{2+} transients. Moreover, the effect of ACE administration is similar to that of nicotine.

Measuring the tissue concentrations of ACE and its metabolites

We measured the concentrations of ACE and its metabolites in the cerebral cortex, hippocampus, striatum, liver, and blood of mice in groups C and A 1 h after ACE administration (Table 3).

We could not detect ACE and its metabolites in group C. ACE and dm-ACE were detected in all target organs in group A (Table 3). The mean concentrations of ACE in the cortical, hippocampal, striatal, liver, and blood tissues were 8.37 ± 0.53 μg/g, 7.47 ± 0.37 μg/g, 9.04 ± 0.51 μg/g, 19.2 ± 1.1 μg/g and 6.48 ± 0.27 μg/mL respectively. Moreover, the mean concentrations of dm-ACE in the cortical, hippocampal, striatal, liver, and blood tissues were 3.45 ± 0.32 μg/g, 3.39 ± 0.21 μg/g, 3.46 ± 0.14 μg/g, 14.9 ± 0.88 μg/g, and 5.54 ± 0.30 μg/mL, respectively. *N*-acetyl-dm-ACE was also detected in the blood (63.6 ± 0.26 ng/mL). Other peaks with S/N>10 were detected for dc-ACE and *N*-acetyl-dm-ACE in the liver, and in various brain regions and the liver, respectively (Table 3). However, dm-dc-ACE and *N*-acetyl-ACE were not detected in any organ.

Discussion

The oral administration of ACE (20 mg/kg bw) in mature mice with a less than the NOAEL and a tenth or half of the median lethal dose of nicotine (0.33 or 1.65 mg/kg bw, respectively) increased anxiety-like behavior associated with altered activities of the neuronal population in the somatosensory cortex. Furthermore, we detected ACE and metabolites in the brain 1 h after ACE administration.

The transfer of ACE to the brain

ACE acts as an agonist of nAChRs, which are pentameric ligand-dependent ion channels. There are various subtypes of nAChRs. α4β2 hetero-pentamers and α7 homo-pentamers are the most frequently expressed subtypes in the vertebrate brain[29]. The α4β2 and α7 subtypes have two and five acetylcholine binding sites, respectively, where acetylcholine binds to induce the depolarization of the postsynaptic membrane[30]. However, the agonist effects of NNs depend on the type of NN and the nAChR subtype to which it binds. For example, ACE reportedly acts as a partial agonist of the α7 subtype[31].

We observed the distribution of ACE and dm-ACE to the cerebral cortex, hippocampus, and striatum 1 h after the acute oral administration of ACE (Table 3). ACE and its metabolites have been previously detected in the brain[32]. However, no study has measured differences in the concentrations of ACE and its metabolites in different brain regions. Our results provide additional evidence to support the hypothesis that NNs and their metabolites may cross the blood-brain barrier.

NNs generally undergo metabolic activation[2], thus necessitating the pharmacokinetics of not only the parent compound but also its metabolites. The major metabolite detected in the brain and blood was dm-ACE. However, we also detected *N*-acetyl-dm-ACE (Table 3). Based on findings from previous studies that compared NN metabolism in rats, dogs, cats, and humans, dm-ACE, the primary metabolite of ACE, *N*-acetyl-ACE, and *N*-acetyl-dm-ACE are likely to be detected[33]. Cation-π interactions are required for agonists to bind to nAChRs in mammals, but insect nAChRs have cationic sub-sites[2]. NNs have nitro or cyano substituents and are not protonated under physiological conditions. Cationic nicotine and other compounds have a higher affinity for mammalian nAChRs. In contrast, for insect nAChRs, NNs have a higher affinity than nicotine because the substituents of NNs interact with cationic sub-sites[2]. Therefore, these substituents play an important role in establishing selective toxicity to insect nAChRs. Hence, dc-ACE and dm-dc-ACE with deconjugated cyano substituents may have a higher affinity for mammalian nAChRs. However, we failed to detect a significant amount of dc-ACE and dm-dc-ACE, thus suggesting the selective toxicity of metabolites may not be as high as that of the parent compound.

The acute toxicity, pharmacokinetics, and bioaccumulation of NNs and their metabolites by chronic exposure were different from that by acute exposure. The pharmacokinetics of ACE and its metabolites via chronic and maternal exposure need to be examined for the chronic and developmental toxicity of ACE. In addition to ACE, we could detect high concentrations of dm-ACE in mice brain. dm-ACE exerts modulatory effects on nAChRs. Therefore, the aforementioned neuronal disruption might have been partly caused by dm-ACE. This necessitates studying the effect of dm-ACE on neuronal activity and brain function to clarify the contribution of dm-ACE to ACE-mediated neurotoxicity.

Behavioral changes because of ACE exposure

The EPM test is a conflict model in which the curiosity in a novel environment is in equilibrium with anxiety and the fear of exposure to heights in open arms. Moreover, it is widely used for behavioral analysis of rodents[24,25]. Previous studies have shown that exposure to NNs can induce anxiety-like behaviors[3,32]. We observed a significant decrease in the number of entries into the open arms (Fig. 1E), and an increase in anxiety in the ACE group (20 mg/kg bw, p.o.), 1 h after administration. Clothianidin and thiamethoxam activate the α4 or α7 subtypes

of nAChRs in the rat striatum and induce dopamine release[34]. Considering the variation of nAChR sensitivity among different NNs[31], it is unclear if ACE activates α4, α7, or otherwise. Nonetheless, the above-mentioned behavioral changes were the likely result of changes in catecholamines.

In addition, the effects of nicotine exposure on behavior vary, depending on the animal species, age, sex, strain, and dose[26,34,35]. The subcutaneous injection of nicotine into adult male C57BL6/J mice significantly increases anxiety-like behavior at a dose of 0.05 mg/kg but not at a dose of 0.1 mg/kg or 0.25 mg/kg[9]. We observed no significant changes in the low concentration nicotine group (0.33 mg/kg bw, p.o.), 1 h after the treatment. However, there was a significant increase in the distance traveled and the time spent in closed arms (Figs. 1B, D) in the high nicotine group (1.65 mg/kg bw, p.o.). We observed a significant decrease in the number of entries in the open arms and the number of movements between zones (Figs. 1E, G), suggesting an increase in anxiety-like behavior because of ACE exposure. Therefore, the effects of nicotine on the behavior may not be dose-dependent. Low and high doses may increase anxiety-like behaviors. However, medium doses may not cause any behavioral changes. The metabolism of nicotine in mice is extremely rapid. Following an intraperitoneal administration of 1.0 mg/kg, the half-life in the blood and brain was approximately 7 min and 20 min for nicotine and cotinine, respectively. The latter is a major metabolite of nicotine[10]. In addition, when injected subcutaneously, the half-life of nicotine was approximately 20 min[9]. We measured the nicotine group 1 h after the administration to standardize the measurement time for all groups. However, a change in the measurement time may produce different results.

Altered neural activity in the somatosensory cortex

There is a mixture of cell groups whose activity likely increases and decreases with the activation of nAChRs. We roughly divided the mixed cell groups and calculated the AUC of the Ca^{2+} waveform before administration, divided by the number of firings for each cell. Moreover, we divided the cells with AUC greater than and less than the median. We quantified the firing frequency, amplitude, and synchronized firing of neurons in the somatosensory cortex and observed significant changes in one or more of these parameters in all groups (Fig. 2).

Despite no significant change in the firing frequency in Ca^{2+} imaging, cells that changed beyond 2 SD before the treatment were observed in all groups (Fig. 2D, E). Possible reasons for the above-mentioned result are as follows: (I) there was no significant change in firing frequency in the somatosensory cortex, (II) we did not detect any change at the time of measurement, or (III) we could not extract any change by the AUC-based classification. While the amplitude of firing had significantly decreased in the high-AUC cell group of the ACE group (Fig. 2F), it had significantly increased after 30 min in the low-AUC cell group of the nicotine-treated group (Fig. 2G). *In vitro* studies have reported that ACE elicits a lower amplitude Ca^{2+} response than acetylcholine[36]. Our results suggest that ACE causes Ca^{2+} influx through the activation of nAChRs in the somatosensory layers II/III. The synchronization of firing had significantly decreased and increased in the high- and low-synchronized cell groups (Fig. 2H, I). Therefore, the neuronal activity was altered in both the excitatory and inhibitory cells. Despite our research also being an *in vitro* study, nicotine increases the synchronous firing in cultured hippocampi[37]. Moreover, the β4 subtype is required for increased synchrony in the hippocampus[37]. Unlike the hippocampus, the somatosensory cortex does not express the β4 subtype[29]. Hence, the subtype variations might have contributed to the differences in results from previous studies. Interestingly, we observed significant synchronous changes 2 h

after administration in the nicotine group. This is because the half-life of intraperitoneally administered nicotine in mice brain is approximately 7 min and roughly 20 min for its metabolites[10]. Despite not reflecting a direct effect of nicotine on the nAChR somatosensory neurons, the results indicate a secondary effect, such as changes in neurotransmitters in different brain regions.

Relationship between behavior and changes in neural activity

While the amplitude was significantly low in the high-AUC cell group of the ACE group, it was significantly high in the low-AUC cell group of the nicotine group (Fig. 2F, G). The synchrony of firing was significantly altered in all groups (Fig. 2H, I). In contrast, we observed behavioral effects only in the ACE and high nicotine groups. There were no significant effects in the low nicotine group (Fig. 1). Therefore, changes in the amplitude observed in Ca^{2+} imaging of the somatosensory cortex may correlate with changes in anxiety-like behavior but not necessarily with changes in synchrony. The somatosensory cortex plays an important role in the processing of sensory input, and it is a part of the interaction between pain and anxiety[38,39]. The prefrontal cortex and amygdala also play important roles in anxiety[40]. Our results suggested that ACE and nicotine administration altered the neural activity in the somatosensory cortex and induced anxiety-like behavior. However, we could not detect other relevant parameters under the measurement conditions, thus necessitating additional tests. The local injection of the neurotoxin 6-OHDA into the amygdala of mice causes the loss of dopaminergic neurons in the midbrain and an increase in anxiety-like behavior[41], suggesting that catecholamines are deeply involved in anxiety-like behavior. Therefore, it is necessary to administer typical drugs associated with anxiety-like behavior, such as antidepressants and nAChR blockers, and measure catecholamine levels, in addition to Ca^{2+} imaging, to understand the actual in vivo effects of the aforementioned changes.

Increased anxiety-like behavior reportedly occurs with a prenatal exposure to ACE[42]. ACE can be transferred from the mother to child in humans[6]. This necessitates information on its toxicity during developmental stages. There are several reports on the developmental neurotoxicity of ACE. The oral administration of ACE in the prenatal and neonatal periods impairs neurogenesis in the hippocampus and neocortex and induces microglial activation[43,44]. Despite challenges, such as the difficulty of surgery, Ca^{2+} imaging using two-photon microscopy has the potential to detect these disorders and facilitate our understanding of these developmental neurotoxins.

Limitations to the study must be mentioned here. Changes in the brain neuron activity during an acute exposure differed between the ACE and nicotine groups. Therefore, these tests alone are not sufficient to understand the *in vivo* effects of the brain function disturbances. Furthermore, additional Ca^{2+} imaging and neurotransmitter measurements should be conducted in future.

Conclusions

Our results suggest the possibility of behavioral effects even at NOAEL doses. The effects of nAChR agonists on behavior may also be captured by Ca^{2+} imaging using two-photon microscopy. Nonetheless, our results support the role of behavioral tests and Ca^{2+} imaging in detecting disturbances in brain function. This, in turn, suggests that *in vivo* Ca^{2+} imaging by two-photon microscopy is a promising technique to assess the effects of neurotoxicants.

Declarations

Acknowledgments

We are grateful to Ms. Mai Tamba, Ms. Satoko Namba, and Ms. Nagisa Hirano (Laboratory of Toxicology, Faculty of Veterinary Medicine, Hokkaido University) for their technical support. The contribution of the NWU-Water Research Group is @@. We used the English language editing services provided by Editage. This work was supported by the Grants-in-Aid for Scientific Research from the Ministry of Education, Culture, Sports, Science and Technology of Japan, awarded to M. Ishizuka (No. 16H0177906, 18K1984708, 18KK028708, and JPMXS0420100620), Y. Ikenaka (No. 17K2003807 and 18H0413208), N. Hoshi (No. 19H0427719), T. Hirano (No. JP19K19406), and Nakayama (17KK0009). This work was also supported by the foundation of the JSPS Bilateral Open Partnership Joint Research (JPJSBP120209902) and the Environment Research and Technology Development Fund (SII-1/3-2, 4RF-1802/18949907) of the Environmental Restoration and Conservation Agency of Japan. We also acknowledge the financial support from the Soroptimist Japan Foundation, the Nakajima Foundation, the Sumitomo Foundation, the Nihon Seimei Foundation, and the Japan Prize Foundation. This research was also supported by JST/JICA, SATREPS (Science and Technology Research Partnership for Sustainable Development; No. JPMJSA1501) and the Hokkaido University School of Veterinary Medicine Wise/Leading Travel and Subsistence Grant.

Funding This work was also supported by the foundation of the JSPS Bilateral Open Partnership Joint Research (JPJSBP120209902) and the Environment Research and Technology Development Fund (SII-1/3-2, 4RF-1802/18949907) of the Environmental Restoration and Conservation Agency of Japan. We also acknowledge the financial support from the Soroptimist Japan Foundation, the Nakajima Foundation, the Sumitomo Foundation, the Nihon Seimei Foundation, and the Japan Prize Foundation. This research was also supported by JST/JICA, SATREPS (Science and Technology Research Partnership for Sustainable Development; No. JPMJSA1501) and the Hokkaido University School of Veterinary Medicine Wise/Leading Travel and Subsistence Grant.

Conflicts of interest The authors have no conflicts of interest in any content of this article.

Availability of data and material The datasets generated during and/or analysed during the current study are available from the corresponding author on reasonable request.

Authors' contributions Anri Hirai, Shouta Sugio and Yoshinori Ikenaka wrote the main manuscript text.

Collins Nimako, Shouta M.M. Nakayama, Kazutoshi Fujioka, Kumiko Taira and Mayumi Ishizuka measured the concentration of acetamiprid in brain.

Keisuke Kato, Keisuke Takahashi, and Koji Arizono synthesized the metabolites of acetamiprid.

Tetsushi Hirano and Nobuhiko Hoshi conducted behavioral tests.

Anri Hirai, Shouta Sugio, Hiroaki Wake conducted Ca2+ imaging.

Ethics approval All the animal experiments were approved by the Experimental Committee of the Faculty of Veterinary Medicine, Hokkaido University (approval number: 18-0061; validity period: 04/2018-03/2023). The study was carried out in compliance with the ARRIVE guidelines.

References

1. Roberts, J. R., Dawley, E. H. & Reigart, J. R. Children's low-level pesticide exposure and associations with autism and ADHD: a review. *Pediatric Research* vol. 85 234–241 (2019).
2. Tomizawa, M. & Casida, J. E. Neonicotinoid insecticide toxicology: Mechanisms of selective action. *Annual Review of Pharmacology and Toxicology* vol. 45 247–268 (2005).
3. Hirano, T. *et al.* NOAEL-dose of a neonicotinoid pesticide, clothianidin, acutely induce anxiety-related behavior with human-audible vocalizations in male mice in a novel environment. *Toxicol. Lett.***282**, 57–63 (2018).
4. Ueyama, J. *et al.* Temporal Levels of Urinary Neonicotinoid and Dialkylphosphate Concentrations in Japanese Women between 1994 and 2011. *Environmental Science and Technology* vol. 49 14522–14528 (2015).
5. Ikenaka, Y. *et al.* EXPOSURES OF CHILDREN TO NEONICOTINOIDS IN PINE WILT DISEASE CONTROL AREAS. *Environ. Toxicol. Chem.***38**, etc.4316 (2018).
6. Ichikawa, G. *et al.* LC-ESI/MS/MS analysis of neonicotinoids in urine of very low birth weight infants at birth. *PLoS One***14**, (2019).
7. Claudio, L., Kwa, W. C., Russell, A. L. & Wallinga, D. Testing methods for developmental neurotoxicity of environmental chemicals. *Toxicol. Appl. Pharmacol.***164**, 1–14 (2000).
8. EFSA. Evaluation of the data on clothianidin, imidacloprid and thiamethoxam for the updated risk assessment to bees for seed treatments and granules in the EU. *EFSA Support. Publ.***15**, (2018).
9. Akinola, L. S. *et al.* C57BL/6 substrain differences in pharmacological effects after acute and repeated nicotine administration. *Brain Sci.***9**, (2019).
10. Petersen, D. R., Norris, K. J. & Thompson, J. A. A comparative study of the disposition of nicotine and its metabolites in three inbred strains of mice. *Drug Metab. Dispos.***12**, (1984).
11. Hritcu, L., Clicinschi, M. & Nabeshima, T. Brain serotonin depletion impairs short-term memory, but not long-term memory in rats. *Physiol. Behav.***91**, 652–657 (2007).
12. Umeda, T., Isa, T. & Nishimura, Y. The somatosensory cortex receives information about motor output. *Sci. Adv.***5**, (2019).
13. Metherate, R. Nicotinic Acetylcholine Receptors in Sensory Cortex. *Learning and Memory* vol. 11 50–59 (2004).
14. Gray, C. M. Synchronous oscillations in neuronal systems: Mechanisms and functions. *J. Comput. Neurosci.***1**, 11–38 (1994).
15. Eri Ioka. Synchronous firing. *J. Japan Soc. Fuzzy Theory Intell. Informatics***26**, 113–113 (2014).
16. Burwick, T. The binding problem. *Wiley Interdiscip. Rev. Cogn. Sci.***5**, 305–315 (2014).
17. Buzsáki, G. & Watson, B. O. Brain rhythms and neural syntax: Implications for efficient coding of cognitive content and neuropsychiatric disease. *Dialogues Clin. Neurosci.***14**, 345–367 (2012).
18. Koukouli, F. *et al.* Nicotine reverses hypofrontality in animal models of addiction and schizophrenia. *Nat. Med.***23**, 347–354 (2017).
19. Arroyo, S., Bennett, C. & Hestrin, S. Nicotinic modulation of cortical circuits. *Frontiers in Neural Circuits* vol. 8 (2014).
20. EFSA. Peer review of the pesticide risk assessment of the active substance acetamiprid. *EFSA J.***14**, (2016).

21. Food Safety Commission. *Pesticide Expert Committee, Pesticide Evaluation Report Acetamiprid (3rd Edition)*. (2014).
22. Kimura-Kuroda, J., Komuta, Y., Kuroda, Y., Hayashi, M. & Kawano, H. Nicotine-Like Effects of the Neonicotinoid Insecticides Acetamiprid and Imidacloprid on Cerebellar Neurons from Neonatal Rats. *PLoS One***7**, e32432 (2012).
23. Landoni, J. H. de. Nicotine. *INCHEM* http://www.inchem.org/documents/pims/chemical/nicotine.htm#SubSectionTitle:7.2.2 Relevant animal data (1991).
24. Yamaguchi, T., Togashi, H., Matsumoto, M. & Yoshioka, M. Evaluation of anxiety-related behavior in elevated plus-maze test and its applications. *Folia Pharmacol. Jpn.***126**, 99–105 (2005).
25. Walf, A. A. & Frye, C. A. The use of the elevated plus maze as an assay of anxiety-related behavior in rodents. *Nat. Protoc.***2**, 322–328 (2007).
26. Biala, G. & Budzynska, B. Effects of acute and chronic nicotine on elevated plus maze in mice: Involvement of calcium channels. *Life Sci.***79**, 81–88 (2006).
27. Schindelin, J. *et al.* Fiji: An open-source platform for biological-image analysis. *Nature Methods* vol. 9 676–682 (2012).
28. Thévenaz, P., Ruttimann, U. E. & Unser, M. A pyramid approach to subpixel registration based on intensity. *IEEE Trans. Image Process.***7**, 27–41 (1998).
29. Gotti, C., Zoli, M. & Clementi, F. Brain nicotinic acetylcholine receptors: native subtypes and their relevance. *Trends in Pharmacological Sciences* vol. 27 482–491 (2006).
30. Matsuda, K., Ihara, M. & Sattelle, D. B. Neonicotinoid Insecticides: Molecular Targets, Resistance, and Toxicity. *Annu. Rev. Pharmacol. Toxicol.***60**, 241–255 (2020).
31. Cartereau, A., Martin, C. & Thany, S. H. Neonicotinoid insecticides differently modulate acetycholine-induced currents on mammalian α7 nicotinic acetylcholine receptors. *Br. J. Pharmacol.***175**, 1987–1998 (2018).
32. Ford, K. A. & Casida, J. E. Chloropyridinyl neonicotinoid insecticides: Diverse molecular substituents contribute to facile metabolism in mice. *Chem. Res. Toxicol.***19**, 944–951 (2006).
33. Khidkhan, K. *et al.* Interspecies differences in cytochrome P450-mediated metabolism of neonicotinoids among cats, dogs, rats, and humans. *Comp. Biochem. Physiol. Part - C Toxicol. Pharmacol.***239**, 108898 (2021).
34. Faro, L. R. F., Tak-Kim, H., Alfonso, M. & Durán, R. Clothianidin, a neonicotinoid insecticide, activates α4β2, α7 and muscarinic receptors to induce in vivo dopamine release from rat striatum. *Toxicology***426**, 152285 (2019).
35. Rodrigues, K. J. A. *et al.* Behavioral and biochemical effects of neonicotinoid thiamethoxam on the cholinergic system in rats. *Ecotoxicol. Environ. Saf.***73**, 101–107 (2010).
36. Houchat, J. N., Cartereau, A., Le Mauff, A., Taillebois, E. & Thany, S. H. An overview on the effect of neonicotinoid insecticides on mammalian cholinergic functions through the activation of neuronal nicotinic acetylcholine receptors. *International Journal of Environmental Research and Public Health* vol. 17 (2020).
37. Djemil, S. *et al.* Activation of nicotinic acetylcholine receptors induces potentiation and synchronization within in vitro hippocampal networks. *J. Neurochem.***153**, 468–484 (2020).

38. Borich, M. R., Brodie, S. M., Gray, W. A., Ionta, S. & Boyd, L. A. Understanding the role of the primary somatosensory cortex: Opportunities for rehabilitation. *Neuropsychologia***79**, 246–255 (2015).
39. Zhuo, M. Neural Mechanisms Underlying Anxiety-Chronic Pain Interactions. *Trends in Neurosciences* vol. 39 136–145 (2016).
40. Davidson, R. J. Anxiety and affective style: Role of prefrontal cortex and amygdala. *Biological Psychiatry* vol. 51 68–80 (2002).
41. Ferrazzo, S. *et al.* Increased anxiety-like behavior following circuit-specific catecholamine denervation in mice. *Neurobiol. Dis.***125**, 55–66 (2019).
42. Sano, K. *et al.* In utero and lactational exposure to acetamiprid induces abnormalities in socio-sexual and anxiety-related behaviors of male mice. *Front. Neurosci.***10**, (2016).
43. Nakayama, A., Yoshida, M., Kagawa, N. & Nagao, T. The neonicotinoids acetamiprid and imidacloprid impair neurogenesis and alter the microglial profile in the hippocampal dentate gyrus of mouse neonates. *J. Appl. Toxicol.***39**, 877–887 (2019).
44. Kagawa, N. & Nagao, T. Neurodevelopmental toxicity in the mouse neocortex following prenatal exposure to acetamiprid. *J. Appl. Toxicol.***38**, 1521–1528 (2018).

Tables

Table 1 LC/MS parameters for ACE and its metabolites

Compound	RT [min]	MRM Transition [m/z]		CE [V]
		Precursor Ion	Product Ion	
Acetamiprid	3.3	233.1	126.0	24
(ACE)			56.3	16
Acetamiprid-d6	3.3	229.2	125.9	28
(ACE-d6)			62.2	16
Acetamiprid-*N*-desmethyl	3.0	209.1	125.8	20
(dm-ACE)			72.9	52
N-desmethyl-acetamiprid-d3	3.0	212.2	126.2	24
(dm-ACE-d3)			89.9	36
N-descyano-acetamiprid	2.2	198.0	126.1	28
(dc-ACE)			90.1	44
N-desmethyl-descyano-acetamiprid	1.8	184.0	126.1	20
(dm-dc-ACE)			73.0	60
N-acetyl-acetamiprid	3.1	199.0	126.1	20
(*N*-acetyl-ACE)			56.2	20
N-acetyl-desmethyl-acetamiprid	2.7	185.0	126.0	20
(*N*-acetyl-dm-ACE)			107.1	24

Target ion is the product ion listed in the top column of each conpound. Other product ions are used as qualifier ions.

Table 2 LOQ and LOD of ACE and its metabolites

Compound	LOQ [ng/mL]	LOD [ng/mL]
ACE	0.472	0.156
dm-ACE	1.16	0.382
dc-ACE	1.35	0.445
dm-dc-ACE	1.28	0.423
N-acetyl-ACE	0.955	0.315
N-acetyl-dm-ACE	1.02	0.336

Table 3 The concentration of ACE and dm-ACE in organs and blood in acute exposure experiment（mean±SEM, ND = not detected)

Compound	Concentration				
	Cortex [μg/g]	Hippocampus [μg/g]	Striatum [μg/g]	Liver [μg/g]	Blood [μg/mL]
ACE	8.37±0.53	7.47±0.37	9.04±0.51	19.2±1.1	6.48±0.27
dm-ACE	3.45±0.32	3.39±0.21	3.46±0.14	14.9±0.88	5.54±0.30
dc-ACE	ND	ND	ND	0.0795±0.0040	ND
dm-dc-ACE	ND	ND	ND	ND	ND
N-acetyl-ACE	ND	ND	ND	ND	ND
N-acetyl-dm-ACE	0.258±0.0062	0.259±0.0067	0.317±0.042	0.248±0.012	0.0636±0.00026

Table 4 Summary of the neuronal activities in somatosensory cortex

Acetamiprid							
High-AUC group				Low-AUC group			
	Frequency (Hz)	Amplitude ($\Delta F/F_0$)	C.C. of paired neuron		Frequency (Hz)	Amplitude ($\Delta F/F_0$)	C.C. of paired neuron
Pre	0.0261±0.0012	3.53±0.23	0.401±0.058	Pre	0.0273±0.0015	3.20±0.29	0.138±0.0032
30 min	0.0300±0.0040	2.67±0.22	0.293±0.0075	30 min	0.0293±0.0013	2.91±0.22	0.205±0.0046
2 hr	0.0285±0.0015	2.77±0.27	0.278±0.0068	2 hr	0.0301±0.0015	3.14±0.27	0.217±0.0042
Nicotine (low dose)							
High-AUC group				Low-AUC group			
	Frequency (Hz)	Amplitude ($\Delta F/F_0$)	C.C. of paired neuron		Frequency (Hz)	Amplitude ($\Delta F/F_0$)	C.C. of paired neuron
Pre	0.0258±0.0015	3.10±0.45	0.367±0.014	Pre	0.0286±0.0019	2.06±0.27	0.136±0.0065
30 min	0.0223±0.0015	2.66±0.42	0.294±0.016	30 min	0.0302±0.0038	2.75±0.44	0.201±0.013
2 hr	0.0299±0.0028	3.06±0.48	0.246±0.013	2 hr	0.0330±0.0023	2.43±0.39	0.177±0.010
Nicotine (high dose)							
High-AUC group				Low-AUC group			
	Frequency (Hz)	Amplitude ($\Delta F/F_0$)	C.C. of paired neuron		Frequency (Hz)	Amplitude ($\Delta F/F_0$)	C.C. of paired neuron
Pre	0.0301±0.0015	3.65±0.26	0.354±0.0049	Pre	0.0309±0.0021	2.32±0.18	0.113±0.0026
30 min	0.0303±0.0018	4.15±0.40	0.264±0.0068	30 min	0.0312±0.0020	3.04±0.24	0.215±0.0059
2 hr	0.0277±0.0020	3.44±0.27	0.266±0.0067	2 hr	0.0275±0.0019	2.63±0.23	0.209±0.0065

Figures

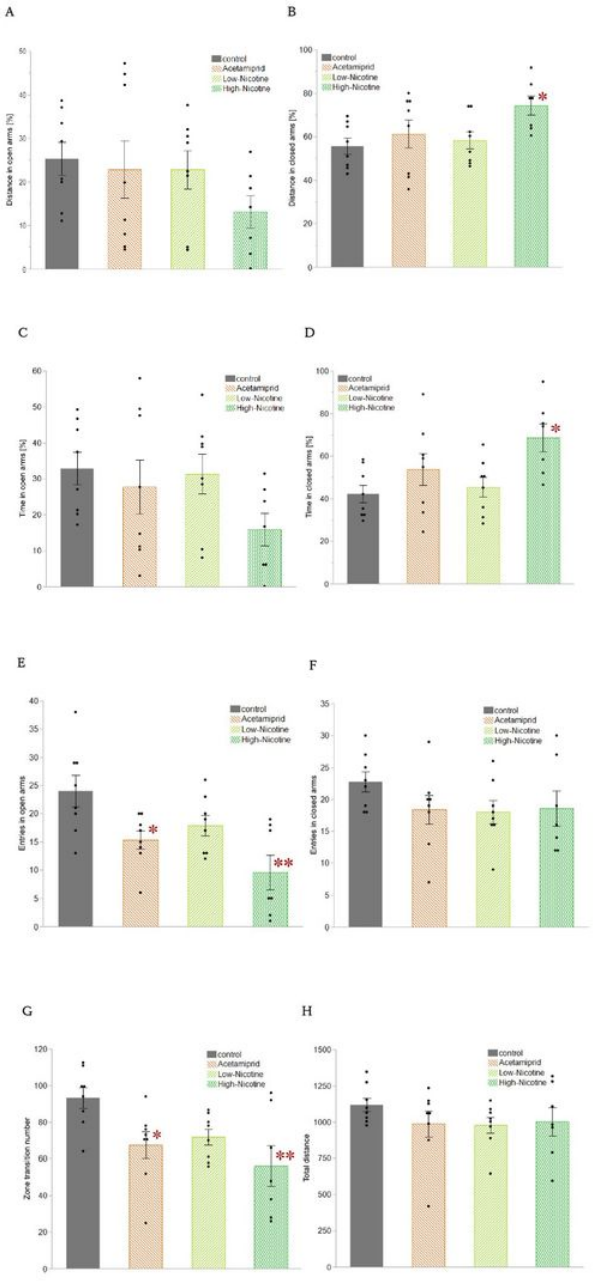

Figure 1

Behavioral effects of acute exposure of 20 mg/kg acetamiprid and 0.33 or 1.65 mg/kg nicotine in the elevated plus-maze (EPM) test (a) Distance traveled in open arms; (b) Time spent in open arms; (c) Entries into open arms; (d) Distance traveled in closed arms; (e) Time spent in closed arms; (f) Entries into closed arms; (g) The number of movements between zones; and (h) Total distance traveled in EPM. Data are represented as mean±SEM, *p<0.05, **p<0.01.

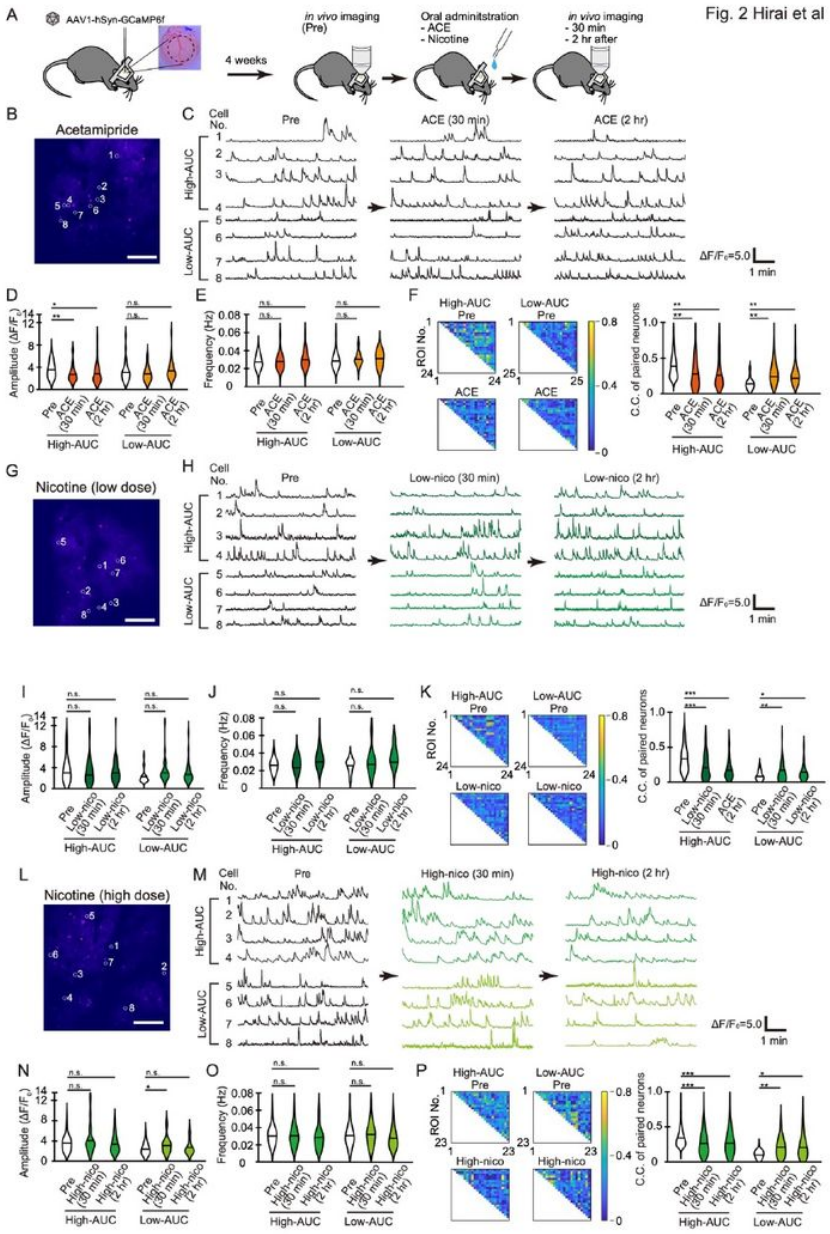

Figure 2

The effect of acute administration of acetamiprid (20 mg/kg, p.o.) and low-dose (0.33 mg/kg, p.o.) or high-dose (1.65 mg/kg, p.o.) of nicotine on the neuronal activity in the somatosensory cortex (a) A schematic drawing of the experimental procedure for the two-photon microscopy. Wild-type mice have been injected adeno-associated virus vector-encoding GCaMP6f into the somatosensory cortex to enable Ca2+ imaging of neurons. In vivo Ca2+ imaging has been performed before and after the oral administration of regents; (b, g, and l) Representative images of neurons expressing GCaMP6f. Typical Ca2+ responses, before and after the administration, recorded from the circled cells and represented in c, h, and m, respectively. Scale bar, 100 μm; (c, h, and m) Ca2+ responses from same neurons; (d, i, and n) The amplitude; (e, j, and o) frequency of Ca2+ transient in each group, before and

after the administration; (f, k, and p) Representative results of correlation co-efficiency for paired neurons. Color-code maps indicate that the typical neuron sets have responded to each reagent. n.s., not significant. *p<0.05, **p<0.01, ***p<0.001.